



Portland General Electric Company
Trojan ISFSI
71760 Columbia River Hwy
Rainier, Oregon 97048

September 29, 2009
VPN-011-2009

Trojan ISFSI
Docket 72-17
License SNM-2509

ATTN: Document Control Desk
Director, Spent Fuel Project Office
Office of Nuclear Material Safety and Safeguards
U.S. Nuclear Regulatory Commission
Washington, DC 20555-0001

Transmittal of Revision 9 to PGE-1069,
Trojan Independent Spent Fuel Storage Installation (ISFSI) Safety Analysis Report (SAR)

Pursuant to 10 CFR 72.70, this letter transmits Revision 9 to Portland General Electric Company's SAR for the Trojan ISFSI. Revision 9 includes changes to the SAR since the last submittal. The Attachment to this letter includes a brief description of the changes included with this revision. Text changes are identified in the SAR by margin bars adjacent to the changes and revision numbers in the page footers.

I hereby certify that Revision 9 accurately presents changes made since Revision 8 necessary to reflect information and analyses prepared pursuant to Commission requirements.

Controlled copy holders are to update their controlled copies per the instructions provided with the enclosure.

Any questions concerning this revision may be directed to Mr. Jay Fischer, of my staff, at (503) 556-7030.

Sincerely,

Stephen M. Quennoz
Vice President
Nuclear & Power Supply/Generation

Attachment
Enclosure

c: Director, NRC Region IV, DNMS
Ms. Shana Helton, NRC, NMSS/DSFST
Thomas M. Stoops, ODOE
Controlled Copy Holders

NMSS01

Summary of Changes Incorporated into Revision 9 of PGE-1069, Trojan ISFSI SAR

The changes incorporated into Revision 9 of the Trojan ISFSI SAR were evaluated in accordance with 10 CFR 72.48 and determination was made that prior NRC approval is not required. Changes summarized below are listed by the Licensing Document Change Request (LDCR) number.

LDCR 2009-001: Implements changes as a result of a revision to the Trojan Damaged Fuel Container structural analysis (Holtec calculation HI-2022869, Revision 3; Trojan calculation TI-149, Revision 1).

1. Section 4.2.4.2.3:
Editorial changes to clarify the damaged fuel container lid is not designed to lift a fuel loaded damaged fuel container.
2. Figure 4.2-5:
Note 3 is added to this figure stating that the fuel loaded failed fuel can may be lifted by the lid.
3. Figure 4.2-5a:
Note 3 is added to this figure stating that the fuel loaded damaged fuel container may not be lifted by the lid.

LDCR 2009-003: Revises Chapter 4 to add a discussion on the MPC lift cleats temperature restriction and its impact on the transfer station operations.

1. Section 4.7.3.4:
A new paragraph, MPC Lift Cleats, is added to the end of this Section to identify that use of the lift cleats are limited to an environment where the ambient air temperature is above 0°F.
2. Section 4.7.4.3:
Adds a new sentence to refer to Section 4.7.3.4 for a discussion on limiting the MPC lift cleat use to an environment where the ambient air temperature is above 0°F.
3. Section 4.9 References:
Adds Reference 34, Holtec PS-1209 Purchase Specification for the MPC Lift Cleat.

LDCR 2009-005: Revises Section 9.8 to reflect a three year delay in fuel shipment and decommissioning, conversion of 1997 dollars to 2008 dollars, and incorporation of TLG Services, Inc. data for the ISFSI Radiological Decommissioning Cost Estimate.

1. Section 9.8.1.2, Decommissioning Schedule:
Editorial changes incorporating the three year delay based on the USDOE's Project Decision Schedule published in January 2009, and adjusting annual O&M costs to 2008 dollars.
2. Section 9.8.2.1, Decommissioning Cost Estimate:
Editorial changes adjusting decommissioning cost estimate to 2008 dollars out to the year 2034, and stating use of guidance document NUREG-1757.
3. Section 9.10, References:
Replaces Reference 3 with NUREG-1757, and deletes Reference 4.
4. Table 9.8-1, ISFSI Radiological Decommissioning Costs:
Revised to incorporate TLG cost estimate data and change to 2008 dollars.

Page 8-40 is corrected to restore existing words that did not print on this page in Revision 8.

Revision 9 to PGE-1069

Trojan Independent Spent Fuel Storage Installation (ISFSI) Safety Analysis Report (SAR)

Revised pages are to be replaced as follows:

REMOVE

Table of Contents

Pages v through vii
Page xiv
Page xviii
Pages xxiii through xxviii

Section 4

Pages 4-7 through 4-20
Pages 4-50 through 4-61
Page 4-73
Figures 4.2-5 and 4.2-5a

Section 8

Page 8-40

Section 9

Pages 9-16 through 9-18
Page 9-20
Table 9.8-1

INSERT

Pages v through vii
Page xiv
Page xviii
Pages xxiii through xxviii

Pages 4-7 through 4-20
Pages 4-50 through 4-61
Page 4-73
Figures 4.2-5 and 4.2-5a

Page 8-40

Pages 9-16 through 9-18
Page 9-20
Table 9.8-1



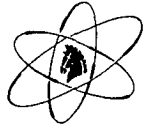
4.0	INSTALLATION DESIGN	4-1
4.1	<u>SUMMARY DESCRIPTION</u>	4-1
4.1.1	LOCATION AND LAYOUT OF INSTALLATION	4-1
4.1.2	PRINCIPAL FEATURES	4-1
4.1.2.1	<u>Site Boundary</u>	4-1
4.1.2.2	<u>Controlled Area</u>	4-1
4.1.2.3	<u>Site Utility Supplies and Systems</u>	4-1
4.1.2.4	<u>Storage Facilities</u>	4-1
4.1.2.5	<u>Stacks</u>	4-1
4.2	<u>STORAGE STRUCTURES</u>	4-2
4.2.1	STRUCTURAL SPECIFICATION	4-2
4.2.2	INSTALLATION LAYOUT	4-3
4.2.2.1	<u>Building Plans and Sections</u>	4-3
4.2.3	CONFINEMENT FEATURES	4-3
4.2.4	INDIVIDUAL UNIT DESCRIPTION	4-4
4.2.4.1	<u>Functional Description</u>	4-4
4.2.4.2	<u>Component Descriptions</u>	4-4
4.2.4.2.1	Description of the MPC	4-4
4.2.4.2.2	Description of the Concrete Cask	4-6
4.2.4.2.3	Failed Fuel Can and Damaged Fuel Container	4-7
4.2.4.2.4	Description of Fuel Debris Process Can and Capsule	4-8
4.2.4.2.5	Component Coatings	4-8
4.2.4.3	<u>Design Bases and Safety Assurance</u>	4-8
4.2.5	STRUCTURAL EVALUATION	4-10
4.2.5.1	<u>Weights and Centers of Gravity</u>	4-10
4.2.5.2	<u>Mechanical Properties of Materials</u>	4-10
4.2.5.3	<u>MPC Stress Analysis Under Normal Loads</u>	4-11
4.2.5.3.1	MPC Thermal Stress Analysis	4-11
4.2.5.3.2	MPC Dead Weight Load Analyses	4-11
4.2.5.3.3	MPC Pressure Analysis	4-11
4.2.5.3.4	MPC Handling Analysis	4-12
4.2.5.3.5	MPC Load Combination	4-12
4.2.5.3.6	MPC Fatigue Evaluation	4-12
4.2.5.3.7	MPC Pressure Test	4-12
4.2.5.3.8	MPC Fracture Toughness	4-13
4.2.5.4	<u>Concrete Cask Analysis Under Normal Operating Loads</u>	4-13
4.2.5.4.1	Concrete Cask Dead Load	4-14
4.2.5.4.2	Concrete Cask Live Load	4-14
4.2.5.4.3	Concrete Cask Thermal Stresses	4-14
4.2.5.4.4	Concrete Cask Load Combination	4-14
4.2.6	THERMAL EVALUATION	4-15



4.2.6.1	<u>Summary of Thermal Properties of Materials</u>	4-16
4.2.6.2	<u>Thermal Models for Normal Storage Conditions-Overview</u>	4-17
4.2.6.3	<u>Global Model of the Trojan Storage System</u>	4-19
4.2.6.3.1	Isotropic Fuel Basket Conductivity	4-19
4.2.6.3.2	Downcomer Gap Conservatism.....	4-20
4.2.6.3.3	Zero (0) Percent Fuel Rods Rupture.....	4-20
4.2.6.3.4	Neglect of Flux Trap Gaps	4-20
4.2.6.3.5	Differences Between the Trojan MPC and the Generic Holtec Design	4-20
4.2.6.3.6	Other Assumptions and Parameters	4-21
4.2.6.4	<u>Concrete Cask Body and MPC Exterior Thermal Model</u>	4-22
4.2.6.5	<u>MPC Thermal Hydraulics</u>	4-23
4.2.6.6	<u>Maximum Temperatures</u>	4-24
4.2.6.7	<u>Minimum Temperatures</u>	4-24
4.2.6.8	<u>Maximum Internal Pressure</u>	4-24
4.2.6.9	<u>Evaluation of Cask Lifetime Performance Under Normal Conditions of Storage</u>	4-24
4.2.7	<u>CRITICALITY EVALUATION</u>	4-25
4.2.7.1	<u>Discussion and Results</u>	4-26
4.2.7.2	<u>Spent Fuel Loading</u>	4-30
4.2.7.2.1	Assembly Classes in HI-STORM Criticality Evaluation.....	4-30
4.2.7.2.2	Spent Fuel Loading at Trojan.....	4-30
4.2.7.3	<u>Model Specification</u>	4-31
4.2.7.3.1	Description of Computational Model	4-31
4.2.7.3.2	Cask Regional Densities.....	4-32
4.2.7.4	<u>Criticality Calculations</u>	4-32
4.2.7.4.1	Criticality Safety Calculations.....	4-32
4.2.7.4.2	Fuel Loading or Other Contents Loading Optimization.....	4-33
4.2.7.4.3	Criticality Results	4-36
4.2.7.4.4	Damaged Fuel and Fuel Debris	4-37
4.2.7.4.5	Fuel Assemblies with Missing Rods	4-39
4.2.7.4.6	Non-fuel Hardware in PWR Fuel Assemblies	4-39
4.2.7.4.7	Neutron Sources in Fuel Assemblies.....	4-39
4.3	<u>AUXILIARY SYSTEMS</u>	4-41
4.3.1	<u>VENTILATION AND OFF-GAS SYSTEMS</u>	4-41
4.3.2	<u>ELECTRICAL SYSTEMS</u>	4-41
4.3.3	<u>AIR SUPPLY SYSTEMS</u>	4-41
4.3.4	<u>STEAM SUPPLY AND DISTRIBUTION SYSTEM</u>	4-41
4.3.5	<u>WATER SUPPLY SYSTEM</u>	4-41
4.3.6	<u>SEWAGE TREATMENT SYSTEM</u>	4-42
4.3.7	<u>COMMUNICATION AND ALARM SYSTEMS</u>	4-42
4.3.8	<u>FIRE PROTECTION SYSTEM</u>	4-42



4.3.9	MAINTENANCE SYSTEMS	4-42
4.3.10	COLD CHEMICAL SYSTEMS	4-42
4.3.11	AIR SAMPLING SYSTEMS	4-42
4.3.12	SEISMIC MONITORING INSTRUMENTATION	4-43
4.4	<u>DECONTAMINATION SYSTEMS</u>	4-44
4.4.1	EQUIPMENT DECONTAMINATION	4-44
4.4.2	PERSONNEL DECONTAMINATION	4-44
4.5	<u>TRANSPORT CASK REPAIR AND MAINTENANCE</u>	4-45
4.6	<u>CATHODIC PROTECTION</u>	4-46
4.7	<u>SPENT FUEL AND HIGH-LEVEL RADIOACTIVE WASTE HANDLING</u> <u>OPERATION SYSTEMS</u>	4-47
4.7.1	STRUCTURAL SPECIFICATIONS	4-47
4.7.2	INSTALLATION LAYOUT	4-48
	4.7.2.1 <u>Building Plans and Sections</u>	4-48
	4.7.2.2 <u>Confinement Features</u>	4-48
4.7.3	INDIVIDUAL UNIT DESCRIPTION	4-48
	4.7.3.1 <u>Transfer Cask Description</u>	4-48
	4.7.3.2 <u>Transfer Station</u>	4-49
	4.7.3.3 <u>Air Pad System</u>	4-49
	4.7.3.4 <u>MPC Lift Cleats</u>	4-49
	4.7.3.5 <u>Mobile Cranes</u>	4-50
4.7.4	STRUCTURAL ANALYSIS OF THE FUEL HANDLING COMPONENTS	4-51
	4.7.4.1 <u>Transfer Cask Lift</u>	4-51
	4.7.4.1.1 <u>Lifting Trunnions</u>	4-51
	4.7.4.1.2 <u>Transfer Cask Wall</u>	4-52
	4.7.4.1.3 <u>Shield Door Rail and Welds</u>	4-53
	4.7.4.1.4 <u>Welds Attaching the Rails to Transfer Cask Shell</u>	4-55
	4.7.4.1.5 <u>Top Lid</u>	4-56
	4.7.4.1.6 <u>Top Lid Bolts</u>	4-56
	4.7.4.2 <u>Air Pad System</u>	4-57
	4.7.4.3 <u>MPC Lift Cleats</u>	4-58
4.7.5	THERMAL EVALUATION DURING FUEL TRANSFER	4-58
	4.7.5.1 <u>Transfer Cask Heat Transfer Modes</u>	4-59
	4.7.5.2 <u>Vacuum Drying</u>	4-59
	4.7.5.2.1 <u>MPC In-Plane Resistance</u>	4-60
	4.7.5.2.2 <u>Gas Conductivity Under Near Vacuum Conditions</u>	4-60
	4.7.5.2.3 <u>Cask Heat Losses to Ambient</u>	4-61
4.8	<u>MATERIALS</u>	4-62
4.9	<u>REFERENCES</u>	4-71



9.8.2.2.2	EWEB/BPA Funding	9-18
9.8.2.2.3	PP&L Funding.....	9-18
9.8.3	RECORD KEEPING FOR DECOMMISSIONING	9-18
9.9	<u>NUCLEAR LIABILITY INSURANCE</u>	9-19
9.10	<u>REFERENCES</u>	9-20
10.0	OPERATING CONTROLS AND LIMITS	10-1
11.0	QUALITY ASSURANCE	11-1



LIST OF TABLES

TABLE	TITLE
7.4-1	Maximum Expected Dose Rates for the Storage Cask System (42,000 MWD/MTU and 9-Year Cooling)
7.4-2	Normal Condition Effluent Dose Calculation Results for the Fully Loaded Trojan ISFSI
7.4-3	Estimated Personnel Doses while Operating the Cask System (42,000 MWD/MTU and 9-Year Cooling)
7.4-4	Dose Rates at the Controlled Area Boundary and Nearest Resident from Effluent and Direct Radiation During Normal and Off-Normal Conditions
8.0-1	Design Basis Normal and Off-Normal Events
8.0-2	Design Basis and Beyond Design Basis Infrequent (Accident) Events
8.1-1	MPC Stresses (ksi) Resulting From Off-Normal Handling Event
8.1-2	Deleted
8.1-3	Summary of Impact from Off-Normal Operations
8.1-4	Release Fractions for Confinement Evaluation of Off-Normal and Accident Conditions
8.2-1	MPC Stresses/Loads Resulting from Accident Pressurization
8.2-2	Off-Normal and Hypothetical Accident Confinement Dose Calculations (Single Cask)
8.2-3	Regulatory Guide 1.76 Design Basis Comparison
8.2-4	Tornado Missile Probability Data
8.2-5	Parameters for Accident Conditions
8.2-6	Bounding χ/Q Values for the Controlled Area Boundary and Nearest Residence for Accident Conditions
8.3-1	Summary of Site Characteristics Affecting the Safety Analysis
9.1-1	ISFSI Staffing Qualifications
9.8-1	ISFSI Radiological Decommissioning Costs



LIST OF EFFECTIVE PAGES

<u>Page Number</u>	<u>Revision</u>
Table of Contents i	7
Table of Contents ii through iv	4
Table of Contents v through vii	9
Table of Contents viii	4
Table of Contents ix and x	7
Table of Contents xi	4
Table of Contents xii and xiii	8
Table of Contents xiv	9
Table of Contents xv through xvii	4
Table of Contents xviii	9
Table of Contents xix	5
Table of Contents xx through xxii	4
Table of Contents xxiii and xxviii	9
1-1 through 1-6	4
1-7	6
Figure 1.1-1	4
Figure 1.3-1	2
Appendix 1.A	4
Drawing 3969	2
Drawing 3970	5
PGE-002	2
Drawing 3971	2
2-1	7
2-2	6
2-3 and 2-4	7
2-5 through 2-7	2
2-8 through 2-10	8
2-11	7
2-12 through 2-15	8
2-16	2
2-17	7
2-18	8
2-19	7
2-20	5
2-21	8
2-22 through 2-27	2



LIST OF EFFECTIVE PAGES

<u>Page Number</u>	<u>Revision</u>
2-28	5
2-29	6
2-30 through 2-33	2
2-34	7
2-35 and 2-36	2
2-37	6
2-38 through 2-42	2
2-43	4
2-44	8
2-45	2
2-46	6
2-47	2
Table 2.1-1	0
Table 2.1-2	0
Table 2.2-1	2
Table 2.7-1	2
Figure 2.1-1	4
Figure 2.1-2	7
Figure 2.1-3	4
Figures 2.1-4 through 2.1-6	0
Figures 2.2-1 and 2.2-2	0
Figures 2.3-1 through 2.3-6	0
Figure 2.4-1	0
Figure 2.4-2	8
3-1 through 3-5	4
3-6	6
3-7 through 3-14	4
3-15	5
3-16	4
3-17	5
3-18	6
3-19	5
3-20	8
3-21	7
3-22 through 3-24	2
3-25	5
Table 3.1-1	0



LIST OF EFFECTIVE PAGES

<u>Page Number</u>	<u>Revision</u>
Tables 3.1-2 and 3.1-3	2
Table 3.1-4	0
Tables 3.2-1 through 3.2-3	0
Tables 3.2-4 and 3.2-5	2
Table 3.2-6	0
Tables 3.6-1 and 3.6-2	2
4-1 through 4-6	4
4-7 through 4-20	9
4-21	5
4-22 through 4-24	4
4-25 and 4-26	5
4-27 and 4-28	4
4-29 through 4-34	5
4-35	4
4-36 and 4-37	5
4-38 through 4-48	4
4-49	8
4-50 through 4-61	9
4-62 through 4-66	4
4-67	8
4-68 through 4-71	4
4-72	5
4-73	9
Tables 4.2-1 and 4.2-2	2
Table 4.2-3, Page 1	8
Table 4.2-3, Pages 2 through 4	2
Table 4.2-3, Page 5	6
Tables 4.2-4 and 4.2-5	2
Table 4.2-6	0
Tables 4.2-7 and 4.2-8	2
Table 4.2-9	3
Table 4.2-10	0
Table 4.2-11	2
Tables 4.2-12 and 4.2-13	3
Tables 4.2-14 through 4.2-16	2
Table 4.7-1	0
Table 4.7-2	8



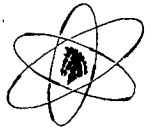
LIST OF EFFECTIVE PAGES

<u>Page Number</u>	<u>Revision</u>
Table 4.8-1	2
Figures 4.2-1a and 4.2-1b	2
Figure 4.2-4	0
Figures 4.2-5 and 4.2-5a	9
Figure 4.2-6a	0
Figure 4.2-6b	0
Figures 4.2-8 through 4.2-16	2
Figures 4.7-1 and 4.7-2	2
Figure 4.7-3	0
Figure 4.7-6	2
Figures 4.7-8 through 4.7-11	2
Figures 4.7-12 through 4.7-13a	3
5-1 through 5-6	4
5-7	6
5-8	4
6-1	4
7-1 and 7-2	4
7-3 through 7-10	5
7-11	6
7-12 through 7-14	5
7-15 and 7-16	7
7-17 and 7-18	4
7-19	7
7-20	4
7-21	6
7-22	4
7-23 through 7-33	7
Tables 7.2-1 through 7.2-3	2
Table 7.2-4	0
Tables 7.2-5 through 7.2-10	2
Table 7.2-11	7
Tables 7.2-12 through 7.2-14	2
Tables 7.3-1 through 7.3-9	2
Table 7.4-1	2
Table 7.4-2	7
Table 7.4-3	4
Table 7.4-4	7



LIST OF EFFECTIVE PAGES

<u>Page Number</u>	<u>Revision</u>
Figure 7.2-1	0
Figures 7.3-1 through 7.3-11	2
8-1	6
8-2	4
8-3	6
8-4 through 8-6	5
8-7	7
8-8 and 8-9	6
8-10	5
8-11	6
8-12 through 8-24	4
8-25	7
8-26 through 8-28	4
8-29 and 8-30	5
8-31	8
8-32	4
8-33 and 8-34	7
8-35	8
8-36 and 8-37	4
8-38	5
8-39	4
8-40	9
8-41 through 8-43	8
Tables 8.0-1 and 8.0-2, Page 1 of 2	2
Table 8.0-2, Page 2 of 2	8
Table 8.1-1	2
Tables 8.1-3 and 8.1-4	2
Tables 8.2-1 and 8.2-2	2
Tables 8.2-3 and 8.2-4	0
Table 8.2-5	2
Table 8.2-6	7
Table 8.3-1	8
Figures 8.1-1 and 8.1-2	2
Figures 8.2-1 through 8.2-4	2
Figure 8.2-6	2
9-1	4
9-2 and 9-3	6



LIST OF EFFECTIVE PAGES

<u>Page Number</u>	<u>Revision</u>
9-4	4
9-5 through 9-7	6
9-8	4
9-9 through 9-12	6
9-13 and 9-14	4
9-15	8
9-16 through 9-18	9
9-19	6
9-20	9
Table 9.1-1	8
Table 9.8-1	9
Figure 9.1-1	6
10-1	4
11-1	6



The Concrete Cask was constructed by pouring concrete between a re-usable form and the inner metal liner. The reinforcing bars and air flow embedments were installed and tied prior to pouring.

A summary of fabrication requirements is presented in Table 4.2-2. Alternatives to the ACI Code for the design of the Concrete Cask are listed in Table 4.2-2a. Figure 4.2-4 provides a description of the Concrete Cask.

4.2.4.2.3 Failed Fuel Can and Damaged Fuel Container

Both the Failed Fuel Can and Damaged Fuel Container are designed to contain partial or complete fuel assemblies with damaged or suspect rods. The internal square opening accommodates a fuel assembly without RCCA inserts. The Failed Fuel Can is designed for storage of a fuel rod storage container, fuel debris Process Can Capsules, fuel assembly metal fragments (e.g., portions of fuel rods, grid assemblies, bottom nozzles, etc.), and fuel debris Process Cans that contain fuel debris and fuel assembly metal fragments. The outside dimensions allow the Failed Fuel Can or Damaged Fuel Container to fit in one of the four oversized storage locations within an MPC.

The shells and lids of both the Failed Fuel Can and the Damaged Fuel Container were fabricated from stainless steel. On the bottom of the shell assemblies and in the lids are screened vent holes. The shells contain four holes on the Failed Fuel Can and five on the Damaged Fuel Container. The lids contain four holes for both the Failed Fuel Can and the Damaged Fuel Container. These vent holes enabled moisture removal from the canister. The vent holes also expose the contents of the Failed Fuel Can or Damaged Fuel Container to the helium atmosphere of the MPC.

The Failed Fuel Can lid was bolted in place. The fuel-loaded Failed Fuel Can is designed to be lifted by the lid using a handling tool. The Damaged Fuel Container lid was locked into position with a locking bar, but is not designed to lift a fuel-loaded Damaged Fuel Container. To remove the Damaged Fuel Container from the MPC, the lid is first removed, then the contained fuel assembly is removed using a normal fuel assembly handling tool. The lid is replaced and the Damaged Fuel Container lifted using a handling tool.

The final Failed Fuel Can that was loaded was not completely full. This Failed Fuel Can was loaded with two Process Cans containing remaining loose fuel pellets, fuel assembly bottom nozzles, and other fuel-related debris. A stainless steel spacer was placed in the Failed Fuel Can to fill the remaining space above the stored material.

Figure 4.2-5 provides a description of the Failed Fuel Can. Figure 4.2-5a provides a description of the Damaged Fuel Container.



4.2.4.2.4 Description of Fuel Debris Process Can and Capsule

The Process Can, shown in Figure 4.2-6a, is the container used to process the organic media and fuel debris located in the Spent Fuel Pool. The Process Can is constructed of 300 series stainless steel for corrosion resistance. The Process Can has 5 micron metallic filters in both the can bottom and lid. These filters allow removal of water and organic media by high temperature steam, while retaining the solid residue from the processed media and fuel debris inside the Process Can.

After high temperature steam processing, up to five (5) Process Cans are placed inside the Process Can Capsule shown in Figure 4.2-6b. The Process Can Capsule is constructed of 304 stainless steel for corrosion resistance and is inerted with helium. The Process Can Capsule provides a sealed containment for the fuel debris. The Process Can Capsule is designed to be lifted by normal fuel handling tools.

The Process Cans are also designed to store fuel assembly hardware (non-fuel bearing components) and loose fuel pellets or fragments. These Process Cans are not placed in a Process Can Capsule, but are directly placed inside a Failed Fuel Can. These Process Cans are not processed by high temperature steam because there is no organic media to remove. Water was removed from the Process Can through the metallic filters during the MPC cavity moisture removal process.

4.2.4.2.5 Component Coatings

No component in the MPC is coated. The carbon steel components of the Transfer Cask are coated with an epoxy-based material suitable for borated water service, as follows:

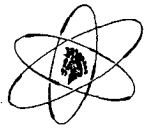
- Primer – Keeler & Long 6548/7107 White Epoxy Primer
- Top Coat – Keeler & Long E-1-7155 Epoxy Enamel

The Transfer Cask coating prevents corrosion and aids in surface decontamination. Sealing surfaces, wear surfaces, gap flush supply line inner surfaces, threaded holes, plugs, and seals are not coated since the coating could affect their ability to perform their design functions.

The coating that has been applied to the carbon steel components of the Trojan Concrete Casks is Carboline Carbozinc 11 VOC. See Section 4.8 for additional discussion of materials used in the Trojan Storage System.

4.2.4.3 Design Bases and Safety Assurance

The design codes for the individual storage structures and components are provided in Section 4.2.1. The storage structures and components are designed for safe long-term storage of spent nuclear fuel. They are designed to survive normal, off-normal, and postulated accident



conditions without release of radioactive material or excessive radiation exposure to workers or members of the general public. Storage systems and components are designed and fabricated in accordance with recognized codes and standards that provide ample safety margin.

Design features that have been incorporated in the ISFSI to provide safe long-term fuel storage include:

1. Leak-tight welds on each MPC shell, baseplate, lid, vent and drain port cover plates, and closure ring,
2. Thick MPC lid to minimize radiation exposure to the public and site personnel,
3. Design of MPC body and internals to withstand a postulated drop accident during storage or transportation, and
4. Design of Concrete Cask to provide radiation shielding of the public and operations personnel, and to protect the MPCs from postulated environmental events.

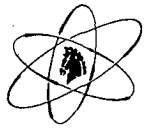
Methods used to minimize personnel radiation exposure during ISFSI operations are discussed in Chapter 7.

Design features to maintain subcritical conditions for normal operations and credible accident scenarios are discussed in Section 4.2.7.

10 CFR 72.126(a)(3) requires access to areas of potential contamination or high radiation within an ISFSI to be controlled. During normal storage conditions, if high radiation areas are identified, they will be controlled in accordance with ISFSI Technical Specification 5.6.1. Increased radiation levels are possible during component handling evolutions. Although not anticipated, any contamination associated with ISFSI operations should be limited to the Storage Pad. The Storage Pad is located in the Protected Area which is surrounded by a security fence. Access to this area is controlled by security and is discussed in Section 3.3.5.1. The Radiation Protection Program is discussed in Chapter 7.

The ISFSI is designed to provide safe storage of spent nuclear fuel for 40 years. In the unlikely event that a permanent off-site disposal or storage facility is not available within 40 years, PGE could pursue one of three options. These include: 1) seek relicensing of the present ISFSI based on additional analysis to extend the design life; 2) construct and license a new ISFSI; or 3) transfer the spent nuclear fuel to an off-site temporary storage facility, if available.

Major design requirements are summarized in Table 4.2-3.



4.2.5 STRUCTURAL EVALUATION

This section describes the design and analyses of the principal structural components of the storage system and components under normal operating conditions. The MPC weight calculation was performed assuming an MPC containing 24 intact fuel assemblies, each containing an RCCA. This weight configuration is considered to conservatively bound actual loading configurations. This section describes the methodology and analysis techniques used, and presents the results.

The storage system structural design criteria are specified in Chapter 3. The combinations of normal, off-normal, and accident loadings have been evaluated per ANSI 57.9 for the Concrete Cask and per the ASME Boiler and Pressure Vessel Code, Section III, Division I, Subsection NB for the MPC confinement boundary.

The following components, utilized for normal spent fuel storage operations, are addressed in this section:

1. MPC confinement boundary (shell, baseplate, lid, vent and drain port cover plates, closure ring, and associated welds);
2. MPC fuel basket;
3. Concrete Cask concrete body; and
4. Concrete Cask steel components (reinforcement, liner, cover lid).

In addition, the handling devices analysis is presented in Section 4.7.

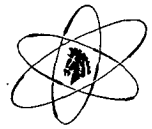
The following sections discuss individual loads and load combinations. The structural evaluations demonstrate that components meet their structural design criteria and are capable of safely storing spent nuclear fuel.

4.2.5.1 Weights and Centers of Gravity

Nominal component weights and centers of gravity for the storage system are summarized in Table 4.2-4 and Figure 4.2-8.

4.2.5.2 Mechanical Properties of Materials

The mechanical properties of steels and concrete used in the structural evaluation of the storage system are consistent with the mechanical properties presented in Tables 4.2-5 and 4.2-6.



4.2.5.3 MPC Stress Analysis Under Normal Loads

4.2.5.3.1 MPC Thermal Stress Analysis

The storage system was evaluated for thermal stresses by using separate and distinct models for the MPC and Concrete Cask. This approach is valid since these components are not structurally coupled. The MPC is free to thermally expand or contract relative to the Concrete Cask. In addition, the fuel basket is not connected to the MPC enclosure vessel so that these components can also be evaluated separately.

For the overall evaluation of the thermal stresses, the temperature distribution for the -40°F ambient condition was used because it causes the highest thermal gradients in the MPC structure. The temperature distribution was obtained from the thermal analysis described in Section 4.2.6.

The MPC internal structure is designed to minimize restrictions of thermal expansion. Existing gaps allow independent expansion of the fuel basket honeycomb and the shell. As a result, thermal stresses in the MPC fuel basket remain low. The thermal stresses for the Trojan Storage System are calculated by scaling the thermal stress analysis results presented in the HI-STAR 100 FSAR (Reference 17) for the generic MPC fuel basket during transport. These analysis results are based on the detailed finite element modeling of the structure. The results are summarized in Table 4.2-7.

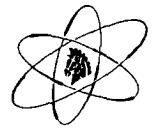
4.2.5.3.2 MPC Dead Weight Load Analyses

The dead weight loads are bounded by the handling loads on the MPC under normal conditions (Level A Service Conditions). The normal handling load on the MPC is assumed to be equal to a 2g acceleration, whereas the dead weight load corresponds to a 1g acceleration. The MPC handling analysis is further discussed in Section 4.2.5.3.4.

4.2.5.3.3 MPC Pressure Analysis

The stresses in the MPC enclosure vessel due to pressure must satisfy the appropriate stress limits from ASME, Section III, Subsection NB. The design basis MPC internal and external pressures under normal operating conditions are 100 psig and 40 psig, respectively. The worst case minimum operating pressure in the MPC exists when an MPC originally loaded with 17.4 kWt cools down to 0 kWt and the ambient temperature drops to -40°F. This pressure is calculated to be 20.2 psig. Table 4.2-9 presents the results of additional cases analyzed under normal conditions with no rod failures and various ambient conditions.

The stress results due to the design basis MPC internal pressure, as well as the results for the combined pressure plus handling loads, are evaluated in Table 4.2-8. The accident pressurization analysis is discussed in Section 8.2.6. Additional calculations have been performed in support of the generic Holtec MPC design to demonstrate that the MPC will not buckle due to design or accident external pressure (Reference 17, Appendix 3.H).



4.2.5.3.4 MPC Handling Analysis

The MPC normal handling load has been defined as 2g applied in the horizontal or vertical direction (Reference 17, Section 3.4.4.3.1.1). The stresses in the MPC due to lateral handling loads are calculated using finite element analysis. The analysis is presented in Section 8.2, and the results are added to the stresses due to the other design loadings in Table 4.2-8. Specifically, the stresses due to the handling load are combined with stresses due to the design basis internal pressure. The combined results are listed in Table 4.2-8 under the column heading "Normal Handling."

4.2.5.3.5 MPC Load Combination

The MPC design loadings are based on dead weight, thermal, internal pressure (not applicable to MPC fuel basket internals), and handling loads. The stresses due to the loadings are presented and evaluated in Table 4.2-8. The first column of results, which is labeled as "Design Internal Pressure," reports the maximum stresses in the MPC enclosure vessel due solely to design internal pressure. The next column ("Normal Handling") provides the maximum stresses in the MPC due to the combined effect of internal pressure plus handling loads. Note that the dead weight of the MPC is considered part of the normal handling load, which is defined as a 2g acceleration.

Since the fuel basket can expand freely under the most severe accident condition thermal gradient, the thermal loads do not contribute to the primary stress levels in the MPC. The thermal stresses in the MPC, which are classified as secondary stresses, are reported in Table 4.2-7. Bounding reference temperatures are used, however, to determine the ASME stress limits in Table 4.2-8. It can be seen that all stresses are within allowable limits.

4.2.5.3.6 MPC Fatigue Evaluation

The passive non-cyclic nature of dry storage conditions does not subject the MPC to conditions that might lead to structural fatigue failure. Ambient temperature and insolation cycling during normal dry storage conditions and the resulting fluctuations in MPC thermal gradients and internal pressure is the only mechanism for fatigue. These low stress, high-cycle conditions can not lead to a fatigue failure of the MPC, which is made from stainless alloy stock (endurance limit well in excess of 20,000 psi). All other off-normal or postulated accident conditions are infrequent or one-time occurrences that cannot produce fatigue failures. Finally, the MPC uses materials that are not susceptible to brittle fracture.

4.2.5.3.7 MPC Pressure Test

The MPC was hydrostatically tested to meet the requirements of ASME Section III, Subsection NB, Article NB-6000 (with Table 4.2-1a alternative), after fuel loading and lid welding were successfully completed. For pressurized conditions, maximum primary stresses



occur in the MPC shell and baseplate. These stresses calculated at a maximum normal design internal pressure of 100 psig are:

Shell

$$P_m = 6.86 \text{ ksi} \quad (\text{ASME Service Level A Limit } 18.7 \text{ ksi at } 400^\circ\text{F})$$

$$P_L + P_b = 10.6 \text{ ksi} \quad (\text{ASME Service Level A Limit } 30.0 \text{ ksi at } 300^\circ\text{F})$$

Baseplate

$$P_m = 2.28 \text{ ksi} \quad (\text{ASME Service Level A Limit } 20.0 \text{ ksi at } 300^\circ\text{F})$$

$$P_L + P_b = 20.5 \text{ ksi} \quad (\text{ASME Service Level A Limit } 30.0 \text{ ksi at } 300^\circ\text{F})$$

Where:

P_m = general primary membrane stress intensity

P_L = local primary membrane stress intensity

P_b = primary bending stress intensity

Table 4.2-8 summarizes the results of maximum stress evaluations for the MPC. In Table 4.2-8, the ASME Service Level A Limits for the MPC shell and baseplate are conservatively evaluated at 450°F and 400°F, respectively.

4.2.5.3.8 MPC Fracture Toughness

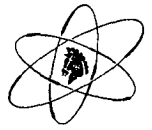
The MPC confinement boundary materials are made of austenitic stainless steel and are exempt from impact testing per ASME, Section III, NB-2311.

The MPC fuel basket structural components are made of austenitic stainless steel. ASME, Section III, NG-2311 exempts austenitic stainless materials from impact testing requirements.

4.2.5.4 Concrete Cask Analysis Under Normal Operating Loads

Three load components act on the Concrete Cask during normal operation: dead load, live load and thermal load due to differential thermal expansion. These components are analyzed below. The results of combining the loads and comparing the Concrete Cask stress levels to allowable limits are summarized in Table 4.2-10. As shown in this table, the Concrete Cask meets the structural requirements of ANSI 57.9 and ACI-349.¹

¹ Refer to Section 4.2.4.2.2 for justification for deviation from ACI-349 temperature limits.



4.2.5.4.1 Concrete Cask Dead Load

The stress due to the dead load (f_D) on the Concrete Cask bottom is conservatively calculated by assuming the total weight of the fully loaded Concrete Cask (300,000 lbs which bounds the weight of the Concrete Cask and the maximum weight of a loaded MPC) is taken by the concrete bottom only over a 12 inch wide area of the bottom plate. The stress is calculated to be 200 psi.

4.2.5.4.2 Concrete Cask Live Load

The Concrete Cask is subject to two live loads: the snow and ice load and the weight of a Transfer Cask and fully loaded MPC during initial cask loading operations. The snow load is uniformly distributed over the top of the Concrete Cask and represents a negligible contribution to Concrete Cask stress levels.

To calculate the stress due to the loaded Transfer Cask, it is assumed that the weight of the loaded Transfer Cask is taken by the steel liner and then by the Concrete Cask bottom. The stress in the steel liner is about 9,746 psi compression. The stress in the bottom (at the Concrete Cask center contact strip) is about 132 psi compression, which also represents a negligible contribution to Concrete Cask stress levels.

4.2.5.4.3 Concrete Cask Thermal Stresses

The Concrete Cask thermal stress is calculated based on the temperature gradient across different components. The Concrete Cask wall analysis is based on the standard approach to concrete which assumes that it resists only compression with steel reinforcement resisting tension. Stresses are calculated by balancing tension and compression in the section because thermal loading can not produce any resultant force.

The thermal stresses in the Concrete Cask are calculated using a conservative temperature gradient of 104°F, which bounds the results for the normal and off-normal ambient conditions and the maximum anticipated heat load thermal gradient of 91°F as shown in Table 4.2-12 for the 12-hour maximum thermal accident condition. The bounding thermal stresses for each of the Concrete Cask structural components are listed in Table 4.2-11. The acceptability of these thermal stress levels is included in the Concrete Cask load combination evaluated in Table 4.2-10.

4.2.5.4.4 Concrete Cask Load Combination

The evaluation of Concrete Cask load combinations in accordance with ACI-349 and ANSI 57.9 is presented in Table 4.2-10. Load combinations 5, 6, and 8 include results of the accident analysis discussed in Chapter 8. For load combination 8, the thermal loads in the critical sections are zero due to the self-balancing nature of the thermal stresses across the entire Concrete Cask section which resists the tornado missile impact. For load combination 6, the thermal stresses



from Table 4.2-11 are recalculated into a moment using the standard technique for concrete analysis.

4.2.6 THERMAL EVALUATION

This section presents the thermal analysis of the storage system for normal operation. Section 4.7.5 provides a detailed discussion of the thermal evaluation of vacuum conditions experienced during initial cask loading.

The significant thermal design feature of the storage system is the air flow path used to remove the maximum of 17.4 kWt of decay heat. This natural circulation of air inside the Concrete Cask allows the concrete temperatures to be maintained below the design limits and keeps the long term fuel cladding temperatures below limits where degradation might occur.

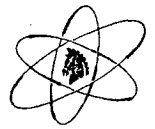
The base calculation was performed assuming 75°F ambient conditions to model the average long term temperatures expected over the life of the Concrete Cask (Reference 30). To include the effect of solar heating under long-term normal storage, appropriately selected insolation inputs are included in the thermal modeling. The inputs are based on assumptions that are in the aggregate selected to assure that the time-averaged solar energy absorbed by a cask over the duration of fuel storage is maximized. For this purpose, the solar absorbtivity is set to a theoretical maximum of unity with sunshine 12 hours per day all days of the year (i.e. clouds, fog, and haze ignored). The insolation energy inputs to the thermal model are:

- Concrete Cask Lid: 387 W/m²
- Concrete Cask Cylinder: 83 W/m²

To bound the expected temperature ranges in which the storage system might operate, two off-normal severe environmental temperature conditions were evaluated (Reference 30). These calculations are presented in Section 8.1.2. The cases considered are -40°F with no solar loads and 100°F with maximum solar loads. The maximum solar load was calculated to be the 24-hour average solar load to model the steady state temperature expected from long term (four to five days) exposure to 100°F air.

The 75°F ambient conditions are utilized to determine long term storage temperatures and -40°F and 100°F ambient temperatures are used to model extreme environmental conditions. In addition to these three cases, one off-normal and two hypothetical accident conditions are analyzed (Reference 30). The off-normal condition considers blockage of one-half of the air inlets, and is addressed in Section 8.1.2. The first hypothetical accident is analyzed as presented in Section 8.2.2, and considers a 125°F ambient condition with maximum solar loads and a maximum decay heat generation. The final analysis, also a hypothetical accident condition, considers the complete blockage of all air inlets. This analysis is addressed in Section 8.2.7.

Table 4.2-12 summarizes the results of the thermal calculations.



4.2.6.1 Summary of Thermal Properties of Materials

The thermal properties used in the thermal hydraulic analyses (Reference 30) are shown in Table 4.2-13. The derived parameters (effective thermal conductivities) are discussed in Section 4.2.6.3, Section 4.2.6.5, and Reference 16. Low values derived from the open literature and conservative calculations were used.

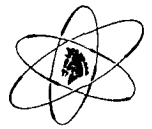
Temperature limits were established for the materials used in the storage system. Specifically, these limits are for concrete, steel, and fuel cladding. The limits were established in accordance with the following:

<u>Source</u>	<u>Component</u>
PNL-6364 Report and BFS analysis (long term) NUREG-1536/PNL-4835 (short term)	Fuel
ASME Section III	Steel
ACI-349 ²	Concrete

Based upon evaluation of these limits it was determined that the fuel cladding and concrete temperature limits were the limiting conditions. Table 4.2-12 presents more details on the long-term and short-term temperature limits for the concrete. While the concrete limit is based on ACI-349, Appendix A, the fuel cladding temperature limit is actually a complex function of temperature versus time, and internal rod pressurization (Reference 2). The limit is established to keep the probability of cladding breach less than 0.5 percent per fuel rod over a 40-year storage term. Using the methodology presented in Reference 2, the fuel cladding allowable temperature limit for normal steady-state conditions was determined to be 341.7°C (647°F) for a Westinghouse 17 x 17 fuel assembly and a minimum cooling time of nine years. The 341.7°C (647°F) limit was determined to bound the B&W 17 x 17 fuel assemblies, which will also be stored in the ISFSI. A short-term temperature limit of 570°C (1058°F) is established for off-normal and accident limits.

In order to determine the applicability of the 1058°F short-term limit for spent fuel clad temperature in NUREG-1536, the Trojan spent fuel was compared to that fuel on which the temperature limit was based. According to PNL-4835, "Technical Basis for Storage of Zircaloy-Clad Spent Fuel in Inert Gases," the spent fuel on which 1058°F was based had a burnup of 28,000 MWD/MTU. The hoop stresses on the spent fuel rods that were tested ranged from approximately 25 MPa to 140 MPa. The maximum hoop stresses in the most limiting Trojan spent fuel rods (i.e., the fuel rods with the highest internal pressure and highest burnup) were within this range indicating that the Trojan fuel is comparable to the fuel rods tested on which the 1058°F temperature limit is based.

² Refer to Section 4.2.4.2.2 for justification for deviation from ACI-349 temperature limits.



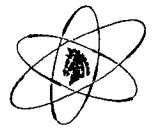
4.2.6.2 Thermal Models for Normal Storage Conditions - Overview

The Trojan Storage System cask configuration consists of a sealed canister (MPC-24E or MPC-24EF, which are identical from a thermal standpoint and are collectively referred to as “MPC” in this discussion) emplaced in a vertically oriented TranStor™ Concrete Cask. In this configuration, a column of air in the canister-to-cask annular gap is thermally connected to the ambient air via top and bottom openings in the Concrete Cask. The canister decay heat elevates the temperature of air in the annulus causing it to rise. The upward air movement draws cold ambient air from the bottom inlets, which is heated by the canister shell in its upward travel and vented from the top ducts. In this manner, a continuous supply of air to the annulus is sustained without any aid of mechanical means, and the canister external surface is cooled by the movement of annulus air as long as there is heat in the canister. Within the MPC, certain features are engineered in the design for dissipating heat from the fuel stored in the cavity space. These features include a welded fuel basket construction and natural circulation convective heat transfer.

The MPC contains an all-stainless steel, full length welded honeycomb basket structure with square-shaped compartments of appropriate dimensions to allow insertion of the fuel assemblies prior to welding of the MPC lid and closure ring. Each box panel is equipped with a Boral (thermal neutron absorber) panel sandwiched between an alloy steel sheathing plate and the box panel, along the entire length of the active fuel region.

The MPC was backfilled with helium to provide a stable, inert environment for long-term storage of the spent nuclear fuel. The helium backfill gas is an integral part of the MPC thermal design that fills all the spaces between solid components. To ensure that the helium gas is retained, the MPC confinement boundary is constructed in accordance with the provisions of the ASME B&PV Code Section III, Subsection NB, with certain approved alternatives, as described in Table 4.2-1a.

The MPC fuel basket design features an uninterrupted panel-to-panel thermal connectivity realized by an all-welded honeycomb basket structure. The MPC design incorporates top and bottom plenums with interconnected downcomer paths. The top plenum is formed by the gap between the bottom of the MPC lid and the top of the honeycomb fuel basket, and by elongated semicircular holes (“mouseholes”) in each basket cell wall. The bottom plenum is formed by rectangular shaped mouseholes at the base of all cell walls. The MPC basket is designed to eliminate structural discontinuities (i.e., gaps), which introduce large thermal resistances to heat flow. Consequently, temperature gradients are minimized in the design, which results in lower thermal stresses within the basket. Low thermal stresses are also ensured by an MPC design that permits unrestrained axial and radial growth of the basket. The possibility of stresses due to restraint on basket periphery thermal growth is eliminated by providing adequate basket-to-canister shell gaps to allow for basket thermal growth during heat-up to design basis temperatures.



It is apparent from the geometry of the MPC that the basket metal, the fuel assemblies, and the contained helium mass will be at their peak temperatures at or near the longitudinal axis of the MPC. The temperatures will attenuate with increasing radial distance from this axis, reaching their lowest values at the outer surface of the MPC shell. Conduction along the metal walls and radiant heat exchange from the fuel assemblies to the MPC metal mass would, therefore, result in substantial differences in the bulk temperatures of helium columns in different fuel storage cells. Since two fluid columns at different temperatures in communicative contact cannot remain in static equilibrium, the non-isotropic temperature field in the MPC internal space guarantees the incipience of the third mode of heat transfer: natural convection.

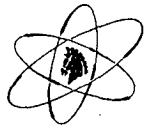
It is recognized that the backfill helium pressure, in combination with low pressure drop circulation passages in the MPC design, induces a thermosiphon upflow through the multi-cellular basket structure to aid in removing the decay heat from the stored fuel assemblies. The decay heat absorbed by the helium during upflow through the basket is rejected to the MPC shell during the subsequent downflow of helium in the peripheral downcomers. This helium thermosiphon heat extraction process significantly reduces the burden on the MPC metal basket structure for heat transport by conduction, thereby minimizing internal basket temperature gradients and resulting thermal stresses.

The helium columns traverse the vertical storage cavity spaces, redistributing heat within the MPC. The holes in the top and bottom of the cell walls, liberal flow space, and wide-open downcomers along the outer periphery of the basket ensure a smooth helium flow regime. The most conspicuous beneficial effect of the helium thermosiphon circulation, as discussed above, is the mitigation of internal thermal stresses in the MPC. Another beneficial effect is reduction of the peak fuel cladding temperatures of the fuel assemblies located in the interior of the basket.

The Trojan cask thermal models employ benchmarked thermal solution methodology. The benchmarking work, documented in a Holtec Topical Report [Reference 16], consisted of simulating experiments carried out by an industry group on a full-scale cask tested in a variety of scenarios (horizontal and vertical orientation, helium and nitrogen filled, and vacuum). The tests used a vertical cask with a 24-cell honeycomb fuel basket containing irradiated PWR fuel (Westinghouse 15x15). The relevance of the benchmarking to cask modeling is established by the employ of a honeycomb basket construction, testing with real life fuel and a reasonably high cask heat load (20.6 kWt).

The thermal modeling methodology features the following constructs:

1. An equivalent conductivity of the fuel assembly situated in a storage cell is computed.
2. The basket/fuel assemblage is simulated as an axisymmetric continuum with an equivalent in-plane conductivity.



3. The hydraulic resistance of the fuel is computed employing the porous media model.
4. The hydraulic resistance of the downcomer space is modeled as an equivalent hydraulic diameter.
5. The space between the fuel basket and MPC shell is modeled as a uniform radial gap filled with helium, as appropriate.

The benchmarking study confirmed that the peak cladding temperature is overpredicted for all test scenarios. The thermal models are summarized in the following sections.

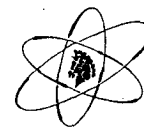
4.2.6.3 Global Model of the Trojan Storage System

The Trojan Storage System thermal solution is produced by a two-step modeling process (Reference 30). In the first step, a Concrete Cask thermal model is constructed to compute the ventilation effect from annulus heating by the MPC decay heat. In this model, heat dissipation from the MPC lid and baseplate is conservatively neglected. In this manner, the annulus heating is maximized, which has the effect of overstating the air, concrete, and MPC shell temperatures. This approach is the same as that employed in the generic HI-STORM 100 thermal modeling (Reference 22, Section 4.4.1.1.9). As an additional measure of conservatism, the MPC shell axial temperature profile is bounded by an Enveloping Linear Variation (ELV). The ELV is employed in the second step in a canister thermal model as a MPC shell temperature boundary condition. From the MPC thermal model, the temperature field of the stored spent nuclear fuel in a pressurized helium environment is obtained.

Axial conduction of heat is considered in the thermal model for both the Concrete Cask concrete and the stainless steel MPC. The FLUENT thermal model includes a finite element representation of certain concrete and stainless steel regions of the cask (e.g., cask concrete cylinder, MPC shell, etc.). Material thermal properties are applied to these finite elements to model conduction heat transfer in accordance with Fourier's Law that states that: (i) heat flow is in the direction of decreasing temperature; and (ii) heat flux is the product of thermal conductivity and temperature gradient. The effect of axial conduction of heat within the finite elements where an axial temperature gradient exists is thus computed and included in the thermal solution. The MPC thermal model employs the benchmarked thermal modeling methodology discussed in Section 4.2.6.2. The principal modeling conservatisms are discussed below.

4.2.6.3.1 Isotropic Fuel Basket Conductivity

It is recognized that the emission of heat in a fuel assembly is axially non-uniform with maximum heat generation in the mid-section of the active fuel length and tapers off toward its extremities. The axial heat conduction in the fuel basket would act to diffuse and levelize the temperature field in the basket. It is also evident that the conduction of heat along the length of the basket occurs in an uninterrupted manner because of a continuously welded honeycomb



structure. On the other hand, in-plane heat transfer is resisted by irremovable gaps that exist between fuel rods, between fuel assembly and basket cell walls. These gaps depress the in-plane conductivity of the basket. In the Trojan thermal modeling, the axial conductivity of the basket/fuel assemblage is set equal to the in-plane conductivity. This assumption has the direct effect of throttling axial heat flow and therefore elevating the temperature of stored fuel.

4.2.6.3.2 Downcomer Gap Conservatism

The MPC basket-to-shell clearance space is modeled as a helium-filled radial gap. This region consists of an azimuthally varying gap formed by the square-celled basket outline and the cylindrical MPC shell. At the locations of closest approach a differential expansion gap (a small clearance on the order of 0.1 inch is engineered to allow free thermal expansion of the basket. At the widest locations, the gaps are on the order of the cell opening (approximately 9 inches). It is evident that heat dissipation by conduction is highest at the closest approach locations and that convective heat transfer is highest at the widest gap locations (large downcomer flow). In the thermal modeling, a radial gap is used that is large compared to the basket-to-shell clearance and small compared to the cell opening. As a relatively large gap penalizes heat dissipation by conduction and a small gap throttles convective flow, the employment of a single gap understates both conduction and convection heat transfer.

4.2.6.3.3 Zero (0) Percent Fuel Rods Rupture

All MPC thermal field calculations are based on a zero percent fuel rods rupture assumption. This minimizes the cavity pressure to understate heat dissipation for fuel temperature calculations. For postulates that require the assumption of large fuel rod ruptures, these temperature fields are grossly overstated.

4.2.6.3.4 Neglect of Flux Trap Gaps

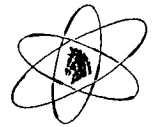
Engineered in the MPC honeycomb basket structure are flux trap gaps between fuel cell walls. These are through-height, open helium flow channels that aid in the removal of heat from the adjacent fuel cells. These helium flow channels are conservatively neglected in the thermal analyses.

4.2.6.3.5 Differences Between the Trojan MPC and the Generic Holtec Design

For accommodating the generic HI-STAR/HI-STORM 100 MPC in a TranStorTM Concrete Cask as opposed to the HI-STAR 100 or HI-STORM 100 overpack, certain changes to the generic MPC design were necessary. These changes are summarized below:

1. Reduced MPC Height

The overall height of the MPC is reduced by about 9 inches to fit the canister in the shorter Concrete Cask cavity.



vertically move the loaded MPC inside the Transfer Cask during MPC transfer between the Transfer Cask and the Concrete Cask or Transport Cask. The lift cleats, attachment hardware, and threaded holes in the MPC lid are designed in accordance with NUREG-0612 and ANSI N14.6 (see Section 4.7.4.3).

The purchase specification for the MPC lift cleats (see Reference 34) limits their use to an environment where the ambient air temperature is above 0°F. If a loaded MPC is placed in the Transfer Cask and the ambient air temperature then drops to or below 0°F, the lift cleats could not be used to raise or lower the MPC, which could pose a safety problem and potential violation of a technical specification. To avoid such a situation, the Transfer Cask will not be used to support a loaded MPC when the ambient temperature is $\leq 10^\circ\text{F}$.

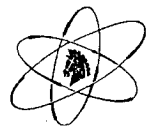
4.7.3.5 Mobile Cranes

The ISFSI design does not include a permanently installed crane, thereby requiring the use of a mobile crane for handling operations. Transferring loaded MPCs at the ISFSI is performed within the specially designed Transfer Station. With the exception of minor boom adjustments to ensure proper alignment of the MPC, the handling of loaded MPCs within the Transfer Station is limited to vertical hook movements to raise the MPC into the Transfer Cask and to subsequently lower the MPC into a Concrete Cask or Transport Cask.

The use of mobile cranes at nuclear power plants is governed in part by ANSI/ASME N45.2.15, with technical requirements specified in ANSI B30.5 (1994). Prior to handling spent fuel casks (i.e. MPCs), procedures for load handling, inspection, safe loads analysis and load tests in accordance with ANSI/ASME N45.2.15 will be in place.

Use of mobile cranes at the Trojan ISFSI will also conform to the guidance in NUREG-0612, "Control of Heavy Loads at Nuclear Power Plants." The use of mobile cranes at the Trojan ISFSI will conform to the guidelines of Section 5.1.1 of NUREG-0612 with the exception that mobile cranes will meet the requirements of ANSI B30.5, "Mobile and Locomotive Cranes," in lieu of the requirements of ANSI B30.2, "Overhead and Gantry Cranes." The mobile crane used at Trojan will have a rated capacity of at least twice the design basis payload, including lifting devices, in accordance with the guidance of Section 5.1.6(1)(a) of NUREG-0612, and will be capable of stopping and holding the load during a Seismic Margin Earthquake (SME).

In addition, the potential drop of a loaded MPC has been evaluated (Reference 26) as described in SAR Section 8.2.13. The structure of the Transfer Station limits potential MPC drops to vertical end drops from within the Transfer Cask into an empty Concrete Cask or Transport Cask. The design of the Transfer Cask precludes lifting the MPC past the top lid of the Transfer Cask. Limit switches or load limiters will be set to minimize the likelihood that the mobile crane will lift the combined weight of the Transfer Cask and MPC from the Transfer Station due to an overlift of the MPC. Nevertheless, the Transfer Cask top lid bolting is designed to ensure the MPC remains inside the Transfer Cask during such an event (see Section 4.7.4.1.5). A specially designed impact limiter in the base of the Transfer Station limits the consequences of this



potential drop. The evaluation of this potential drop conforms to the guidelines of Appendix A to NUREG-0612 and demonstrates that under the postulated drop event:

1. The maximum compressive stress in the enclosure vessel shell is well below the applicable stress limit, and the enclosure vessel does not buckle or exhibit large deformations, such that MPC confinement integrity is maintained after the postulated drop accident;
2. The maximum stress intensities at critical locations (such as the MPC lid-to-shell weld) are well within the Level D service condition limits established in the ASME Code;
3. The maximum stress in the MPC fuel basket is well below the applicable basket stress limit, and the MPC fuel basket structure does not buckle or exhibit large deformations;
4. The stresses in the sheathing welds are below the design basis limits so that the criticality control elements (Boral) will stay in place; and
5. The fuel assembly deceleration is 54g, which is below the 60g design basis deceleration. Therefore, the fuel assemblies will not be damaged such that retrievability would be adversely affected.

4.7.4 STRUCTURAL ANALYSIS OF THE FUEL HANDLING COMPONENTS

4.7.4.1 Transfer Cask Lift

The Transfer Cask is used to support, but not lift, a loaded MPC at the Transfer Station. However, the Transfer Cask was used during initial cask loading operations to lift a load equivalent to a fully-loaded wet MPC. Thus, a loaded Transfer Cask weight of at least 215,000 lbs is used for the lifting device analyses. This is higher than the maximum weight in Table 4.2-4 and, therefore, conservative. Table 4.7-2 provides the results of the stress analysis for the Transfer Cask lift components.

4.7.4.1.1 Lifting Trunnions

The adequacy of the Transfer Cask lifting trunnion design can be evaluated by considering the stress levels in the lifting trunnion and the Transfer Cask wall. The Transfer Cask lifting trunnions are designed with a factor of safety of 10 or greater on ultimate and 6 or greater on yield and includes the dynamic load increase factor of 15 percent.



The maximum shear stress (τ) of the lifting trunnion is:

$$\begin{aligned}\tau &= \frac{(\text{Weight of MPC} + \text{Transfer Cask}) \times 1.15}{(2) \times A_T} \\ &= 4.76 \text{ ksi}\end{aligned}$$

The maximum bending stress (σ_b) in the lifting trunnion is calculated as:

$$\sigma_b = \frac{(\text{Weight of MPC} + \text{Transfer Cask}) \times L \times 1.15}{(2) \times S}$$

where:

L = Distance between face of Transfer Cask trunnion block and mid-point of load application

S = Trunnion section modulus

$$\sigma_b = 16.6 \text{ ksi}$$

The maximum lifting trunnion principal stress (S_I), is determined by combining shear stress and bending stress as follows:

$$\begin{aligned}S_I &= \sigma_b/2 + [(\sigma_b/2)^2 + \tau^2]^{0.5} \\ &= 17.8 \text{ ksi}\end{aligned}$$

Therefore, the factors of safety, ϕ_u (ultimate) and ϕ_y (yield), for the trunnion ($S_u = 181.3$ ksi and $S_y = 147.0$ ksi for SB-637-N07718 steel, at work temperature) are:

$$\phi_u = S_u/S_I = 10.2 > 10$$

$$\phi_y = S_y/S_I = 8.2 > 6$$

Hence, the lifting trunnions are adequate (and meet NUREG-0612-1980/ANSI N14.6-1993) to lift and carry the weight of the Transfer Cask with the MPC fully loaded with fuel and water.

4.7.4.1.2 Transfer Cask Wall

To evaluate the structural integrity of the Transfer Cask wall, an ANSYS finite element analysis was performed with the model shown in Appendix 3.AE of the HI-STORM 100 System FSAR. The model focuses on the Transfer Cask wall region near the lifting trunnion because this is the most critical region. This model is applicable for use in evaluating the Trojan Transfer Cask because the generically certified 100-ton HI-TRAC transfer cask is identical in design in the area



of the lifting trunnions. Only a quarter of the Transfer Cask is modeled due to symmetry. The 3-D "SOLID45" elements are used for the lifting trunnion and Transfer Cask shells.

The primary stresses in the top flange, the inner shell, and the outer shell in the vicinity of the lifting trunnion attachment must not exceed the membrane and membrane plus bending stress limits per the ASME Code, Section III, Subsection NF, for Level A conditions. A bounding weight of 212,500 lbs was assumed in the analysis. The maximum primary stresses in the Transfer Cask wall caused by this bounding load applied at the lifting trunnion are:

$$\text{Max. Primary Membrane Stress, } P_m = 8.14 \text{ ksi}$$

$$\text{Max. Primary Membrane Plus Primary Bending Stress, } P_m + P_b = 10.74 \text{ ksi}$$

Therefore, the factors of safety on this stress are:

$$\begin{aligned} \text{SF (primary membrane)} &= 17.5/8.14 \\ &= 2.15 \end{aligned}$$

$$\begin{aligned} \text{SF (primary membrane plus primary bending)} &= 26.2/10.74 \\ &= 2.44 \end{aligned}$$

In addition, the average stress across the highest loaded section modeled does not exceed one-third of the material yield stress at temperature; this is in keeping with the requirements of Regulatory Guide 3.61.

4.7.4.1.3 Shield Door Rail and Welds

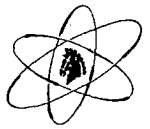
The shield door rails must support the weight of a fully loaded MPC and the weight of the shield doors themselves (a total of approximately 104,200 lbs). The rail design consists of a thick steel plate welded to the bottom of a rectangular solid section of steel. The rail is welded to the bottom plate of the Transfer Cask wall. For the analysis, the rails were assumed to have an overall length of 46 inches (i.e., the supported length of the closed shield doors). The shield door rail design is shown on Figure 4.7-6.

The design load for the rails (considering 15 percent dynamic factor) is

$$\begin{aligned} W &= 104,200 \cdot 1.15 \\ &= 119,830 \text{ lbs} \end{aligned}$$

The structural integrity of the rails is evaluated by first considering the rail bottom plate and its welds. The shear stress in the rail bottom plate due to the applied load of W is:

$$\tau = \frac{W}{2 \times L \times t} = 0.87 \text{ ksi}$$



where:

W = Design load = 119,830 lbs

L = Rail length

t = Rail bottom plate thickness

The maximum bending stress in the rail bottom plate, σ_b , occurs at the section through the inner bottom weld and is calculated below.

$$\sigma_b = M/(Lt^2/6) = (W/2) \times \delta / (Lt^2/6)$$

where:

M = Moment in bottom plate
= (W/2) x δ

δ = Applied load moment arm (1.25 inches)

σ_b = 4.34 ksi

The bottom plate maximum principal stress is then,

$$\begin{aligned} \text{Bottom Plate } S_I &= \sigma_b/2 + [(\sigma_b/2)^2 + \tau^2]^{0.5} \\ &= 4.51 \text{ ksi} \end{aligned}$$

Although the Transfer Cask is designed in accordance with ASME III, Subsection NF, the stress criteria from ANSI N14.6 are applied here for added conservatism. Based on the properties of the material ($S_u = 70$ ksi, $S_y = 34.6$ ksi), the safety factors are:

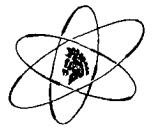
$$\phi_u = 15.5 > 5$$

$$\phi_y = 7.7 > 3$$

The rail lower welds were evaluated by first determining the reactive forces, F_o and F_i , experienced by the outer and inner welds due to the applied load. These forces are found from simple balance of forces and moments.

$$F_o = (\delta/w) \times (W/2) = 13.4 \text{ kips}$$

$$F_i = [(w + \delta)/w](W/2) = 73.3 \text{ kips}$$



where:

w = Distance between welds

Therefore, for the two lower welds the maximum shear stress ($\tau_{\text{lower weld}}$) occurs at the inner groove weld and is calculated as:

$$\begin{aligned}\tau_{\text{lower weld}} &= F_i / (t_{\text{groove}} \times L) \\ &= 3.19 \text{ ksi}\end{aligned}$$

and the maximum principal stress at the weld is (for pure shear condition):

$$\text{Lower Weld } S_I = \tau_{\text{lower weld}} = 3.19 \text{ ksi}$$

Which provides factors of safety of:

$$\phi_u = 22.0 > 5$$

$$\phi_y = 10.9 > 3$$

4.7.4.1.4 Welds Attaching the Rails to Transfer Cask Shell

The load on the weld between the rail and Transfer Cask wall includes the loaded wet MPC as well as the weight of doors and rails for the total of approximately 108,200 lbs (124,430 lbs with a 1.15 load amplification factor). The analysis is done using the standard methodology of treating the weld as a line. The area and section moduli of the weld per one inch of weld throat are calculated to be 83.0 in²/in and 171 in³/in respectively. The center of gravity location is shown in Figure 4.2-8. Then the applied moment (M) is calculated to be 199 kip-in.

Weld force per unit of length (F_w) is calculated as:

$$F_w = (W/2) / A_w + M / S_w = 1.91 \text{ kips/in}$$

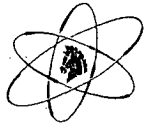
Conservatively assuming a 1/2-inch fillet weld, the stress (f_w) is calculated as:

$$f_w = F_w / (t_w / \%2) = 5.4 \text{ ksi}$$

The ultimate and yield safety factors (ϕ_u and ϕ_y) based on material properties are:

$$\phi_u = S_u / S_I = 13.0 > 5$$

$$\phi_y = S_y / S_I = 6.4 > 3$$



4.7.4.1.5 Top Lid

The purpose of the top lid is to provide radiation shielding and to prevent inadvertent lifting of the MPC out of the Transfer Cask. Therefore, the top lid and its attachment hardware must have sufficient strength to support the weight of an empty Transfer Cask (since an inadvertent MPC lift would cause the lifting of the entire Transfer Cask by the top lid with the load path through the top lid studs). Since this would be an off-normal condition, NUREG-0612 safety factors do not apply and AISC allowable stresses are used for design.

The top lid is a steel ring with a 27-inch diameter center opening. The central opening allows access to the MPC lift cleats when raising or lowering the MPC out of or into the Concrete Cask or Transport Cask. Twenty-four studs and nuts hold the top lid in place.

The stresses on the inner and outer edges, σ_i and σ_o , of the top lid can be calculated using formulas from Reference 10.

The results are:

$$\sigma_i = 2.62 \text{ ksi}$$

$$\sigma_o = 8.73 \text{ ksi}$$

The shear stress on the outer edge of the top lid, τ , is calculated as:

$$\tau = W / 2\pi at = 0.59 \text{ ksi}$$

Therefore, the top lid maximum principal stress due to the applied load is:

$$S_1 = \sigma_o/2 + [(\sigma_o/2)^2 + \tau^2]^{0.5} = 8.77 \text{ ksi}$$

Comparing this stress level to the acceptance criteria shows the top lid is structurally adequate, i.e.,

$$8.77 \text{ ksi} < 26.0 \text{ ksi (0.75}F_y \text{ allowable per AISC)}$$

4.7.4.1.6 Top Lid Bolts

The load on a single bolt due to the reactive force caused by an inadvertent MPC lift is:

$$F_F = W/24 = 5.71 \text{ kips}$$



The load on each bolt due to the bending moment in the lid (prying action) is:

$$F_M = 2\pi a M_r / 24 L = \frac{2\pi a \sigma_o t^2 / 6}{24 \times L}$$

where:

L = Radial distance from outer edge of top lid to bolt circle

M_r = Moment per circumferential length = $\sigma_o t^2 / 6$

t = Top lid thickness

σ_o = 8.73 ksi, see top lid calculation section

a = Bolt circle radius

which after numerical evaluation yields:

$$F_M = 4.56 \text{ kips}$$

Therefore, the tension on each bolt, F, is calculated as:

$$F = F_F + F_M = 10.3 \text{ kips}$$

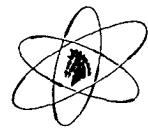
which is within the acceptable range, i.e.,

$$F = 10.3 \text{ kips} < 25.0 \text{ kips (allowable load for 1-inch SA-193 B7 bolt per AISC)}$$

4.7.4.2 Air Pad System

The Concrete Cask may be lifted from below using air pads. This bottom lift is the normal lifting mode. It should be noted that the lift device is not considered important to safety since the Concrete Cask lift is limited to only 3 inches. The air pad system accommodates the fully loaded weight of a Concrete Cask (i.e., Concrete Cask, MPC, 24 fuel assemblies with control components) which is conservatively assumed to be 300,000 lbs. The adequacy of the lift is evaluated by calculating the bearing pressure on the Concrete Cask bottom and comparing it to allowable bearing pressure per ACI-349. Allowable bearing stress is:

$$\begin{aligned} P_b &= \phi(0.85f'_c) \\ &= 0.7(0.85 \cdot 4000) = 2,380 \text{ psi} \end{aligned}$$



The Air Pad bearing pressure is calculated based on the bearing area

$$p = \text{Weight} / (\text{air pad area} - \text{inlet duct area} - \text{air pad area outside of cask envelope})$$
$$= 42.5 \text{ psi}$$

Air pad bearing stresses are negligible. No shear forces or bending moments will exist in the Concrete Cask because the air pads effectively cover the whole bottom area. Hence, the concrete will not crush during a bottom lift of the Concrete Cask.

4.7.4.3 MPC Lift Cleats

The adequacy of the MPC lifting devices is demonstrated by considering each of the MPC lift cleats, the lifting holes and attaching bolts, the MPC lid, and its weld to the shell. The design of the MPC incorporates four (4) threaded holes in the top lid, which accept a pair of MPC lift cleats (refer to Figure 8.2-6). The HI-STAR 100 FSAR (Appendix 3.K of Reference 17) includes an analysis of the lifting holes and an assumed lifting bolt. The MPC lid and lid-to-shell weld are also evaluated in the HI-STAR 100 FSAR for loaded lifting operations. The minimum safety factors for the lid and its peripheral weld are 6.5 and 2.3, respectively. An analysis of the lift cleat is provided here.

The lift cleat is considered as a plane frame structure subjected to a uniform pressure load from the lifting operation. There are two lift cleats, each supporting 50 percent of the lifted load (i.e., the loaded MPC). Frame solutions were used to establish the stress distribution in the lift cleat section. The analysis assumes a dynamic load increase factor of 15 percent.

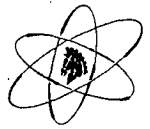
The maximum normal or combined shear stress in each of the lift cleats is limited to the minimum of either 1/10 of the material ultimate strength or 1/6 of the material yield strength for 50 percent of the total lifted load. From the analysis, the minimum safety factor for each MPC lift cleat is 1.04 over and above the 6 and 10 safety factors suggested by ANSI N14.6.

Refer to Section 4.7.3.4 for a discussion on limiting MPC lift cleat use to an environment where ambient temperature is above 0°F.

Section 8.2.13.1.2 analyzes the accident condition in which an MPC overlift results in lifting the Transfer Cask.

4.7.5 THERMAL EVALUATION DURING FUEL TRANSFER

The Transfer Cask model and calculations are presented below (Reference 31). These analyses include conditions in which the loaded MPC is in the Transfer Cask and the MPC cavity consists of a helium atmosphere, and the loaded MPC is in the Transfer Cask and is undergoing vacuum drying operations during initial cask loading. As indicated in Table 4.2-12, the thermal analyses



results associated with the vacuum drying condition bound any other condition anticipated during ISFSI storage and Transfer Station operations, and thus they are retained in this section.

4.7.5.1 Transfer Cask Heat Transfer Modes

Heat is generated in the fuel assemblies and transferred to the Transfer Cask from the MPC surface by radiation and conduction through the air annulus between the MPC and the Transfer Cask in a manner similar to that described in Section 4.2.6.4 for the Concrete Cask and the MPC. The heat is then conducted through the Transfer Cask wall and convected and radiated from its outer surface. The heat transfer modes inside the MPC are the same as discussed in Section 4.2.6.5.

The FLUENT finite volume model similar to that described in Section 4.2.6.4 was used for the analysis. The FLUENT model of the Transfer Cask is depicted in Figure 4.7-8. Ambient temperatures of 75°F and 100°F were used in the analysis.

This analysis determines the temperature distribution in the Transfer Cask and the MPC. Figures 4.7-9 and 4.7-10 show the temperature distribution in the MPC in the Transfer Cask for ambient temperatures of 75°F and 100°F, respectively. Figure 4.7-11 presents the temperature profile through the Transfer Cask wall at the hottest section. The results of the analysis are summarized in Table 4.2-12.

4.7.5.2 Vacuum Drying

Prior to sealing an MPC loaded with fuel, it was dewatered and the residual moisture was removed. Subsequent to the dewatering evolution wherein the bulk of the water in the MPC was displaced by helium or nitrogen, the removal of the remaining moisture was performed by introducing near vacuum conditions within the MPC cavity. Under vacuum drying, the pressure inside the MPC cavity is gradually lowered using a vacuum pump. The fuel decay heat gradually raises the temperature of the MPC contents, which accelerates the drying process. The drying step was followed by backfilling the cavity space with pressurized helium. To determine the peak cladding temperature during the vacuum drying evolution, a thermal analysis was performed (Reference 31). Some of the major assumptions are:

1. Radiation heat dissipation to ambient is understated (Transfer Cask surfaces are assumed unpainted).
2. Heat dissipation in the MPC-to-Transfer Cask annular gap through convection is ignored.
3. Heat dissipation in the water jacket space through convection is ignored.
4. Design maximum cask heat load ($Q = 17.4$ kW) is used.



5. In the reference case thermal evaluation, helium at an MPC cavity pressure of 2 torr is assumed to exist throughout the vacuum drying operation.
6. In the bounding case thermal evaluation, nitrogen at an MPC cavity pressure of 0.5 torr is assumed to exist throughout the vacuum drying operation⁵.

As discussed below, to ensure that the computed temperatures are not grossly overstated, the FLUENT thermal model is appropriately enhanced to eliminate certain overly conservative elements. These are discussed below.

4.7.5.2.1 MPC In-Plane Resistance

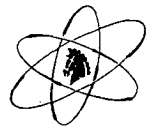
The MPC is rendered as a two-zone axi-symmetric thermal model. An inner zone represents the heat generating fuel basket region. The outer zone is an annular helium/nitrogen-filled region to model the MPC downcomer space. The width of the annular region, sized from hydraulic considerations, overstates the annular gap for conduction heat transfer. Consequently, the in-plane MPC thermal resistance, which is the resultant of fuel basket and downcomer gap resistances, is substantially overstated in the thermal model. The excessive conservatism is ameliorated in the vacuum drying condition by analytically adjusting the inner zone effective conductivity.

4.7.5.2.2 Gas Conductivity Under Near Vacuum Conditions

The thermal conductivity of gases is a very weak function of the concomitant pressure. The conductivity decrease in the low to moderate pressure range is negligible and quite moderate in the ultra low pressure range. In the low to moderate pressure range (10^{-3} bar to 10 bar) (Reference 19), the thermal conductivity drops by about 1 percent for a drop in pressure of 1 bar. Below 10^{-3} bar, conductivity drops in proportion to pressure reduction down to zero. For example, conductivity at 0.5×10^{-3} bar is half the value at 10^{-3} bar. This region is denoted in the technical literature as the Knudsen domain. This domain is approached from above in the vacuum drying operation wherein the pressure is gradually reduced from approximately 760 torr down to below 3 torr for 30 minutes to verify dryness. For the first vacuum calculation, a reference case pressure of 2 torr of helium is evaluated. Employing helium conductivity data at 1 atmosphere pressure (760 torr), the conductivity drop at 2 torr is about 1 percent. For additional conservatism, a 5 percent reduction in helium conductivity is employed in the FLUENT models.

For the second, bounding case using nitrogen, a pressure of 0.5 torr is assumed and the gas conductivity is reduced to conservatively bound the conductivity reduction due to pressure reduction during vacuum drying.

⁵ If nitrogen is used for blowdown, it will contain a small amount of helium from the preceding helium leakage test evolution. However, it is conservative to assume 100 percent nitrogen in the analysis of this case because nitrogen is less conductive than helium.

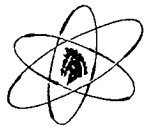


4.7.5.2.3 Cask Heat Losses to Ambient

In this evaluation, heat losses from cask to ambient via natural convection and radiation heat transfer are included. The thermal modeling assumes a Transfer Cask with no credit for increased radiation heat dissipation due to coatings. The ambient temperature is postulated at the normal temperature of 75°F (Table 4.2-12).

Employing the assumptions above at the design maximum heat load of 17.4 kW, a transient thermal model was generated and a 75-hour time-dependent rise in the PCT computed. The start of the transient postulates an MPC with its cavity water heated to normal boiling point followed by an instantaneous dewatering step. Transient PCT plots are shown in Figures 4.7-12 and 4.7-12a for helium and nitrogen, respectively. Several days of vacuum drying are necessary to approach the asymptotic steady state temperature of 659°F (helium) or 711°F (nitrogen).

The above results are applicable for a hypothetical bounding heat load (referred to as the design maximum heat load) of 17.4 kW. In reality, at the beginning of fuel loadings (circa December 2002), the cask heat loads were well below 15 kW. An analysis of the vacuum drying condition with helium and nitrogen under a heat of 15 kW is provided as transient PCT temperature profile shown in Figures 4.7-13 and 4.7-13a. The steady state PCT is closely approached after several days of vacuum drying operation. The asymptotic steady state PCT (rounded to a whole number) is computed as 610°F (helium) and 642°F (nitrogen), both of which are below the long term normal fuel cladding temperature limit of 647°F.



31. Holtec Report No. HI-2012725, "Computation of Peak Cladding Temperature During Vacuum Drying of Trojan Fuel (Trojan ISFSI Completion Project)," Revision 4.
32. Holtec Report No. HI-2012681, "Criticality Evaluation for the Trojan ISFSI Completion Project," Revision 7.
33. Holtec Report No. HI-2012662, "Fuel Parameter Evaluation of TNP Fuel to be Stored at the Trojan ISFSI," Revision 3
34. Holtec PS-1209, Purchase Specification for the MPC Lift Cleat (Ancillary No. 209).

Figure Withheld Under 10 CFR 2.390

TROJAN ISFSI
SAFETY ANALYSIS REPORT

FIGURE 4.2-5
FAILED FUEL CAN

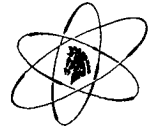
Revision 9

Figure Withheld Under 10 CFR 2.390

TROJAN ISFSI
SAFETY ANALYSIS REPORT

FIGURE 4.2-5a
DAMAGED FUEL CONTAINER

Revision 9



In conclusion, the consequences of the postulated free-fall drop accident of a loaded MPC from a HI-TRAC Transfer Cask into a HI-STAR 100 Transport Cask or Concrete Cask at the Transfer Station satisfy the acceptance criteria.

8.2.13.3.4 Accident Dose Calculation

There are no radiological releases or adverse radiological consequences from this event.

8.2.13.4 Loaded Transport Cask Drop

A vertical or horizontal drop of a loaded Transport Cask is speculated to occur during transfer to a heavy-haul trailer or rail car prior to the installation of transportation packaging impact limiters.

Section 9.7.5 establishes that a program provide the requirements governing handling or lifting fuel bearing components including Transport Casks. Handling/lifting of spent fuel or handling/lifting of loads over spent fuel are performed only in accordance with approved lift plans. An evaluation of consequences of a drop or handling accident shall be performed prior to initiating the handling/lifting activities.

In accordance with the program described in Section 9.7.5, an evaluation to criteria equivalent to those specified in NUREG-0612 will be performed of the entire fuel transfer and loading process. Handling of the Transport Cask at the ISFSI could utilize increased safety factors in the rigging to preclude drops or impact limiters to mitigate the effects of drops prior to installation of the transportation packaging.



9.8.1.2 Decommissioning Schedule

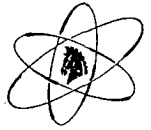
The DOE is responsible for the acceptance of spent nuclear fuel and related nuclear material in accordance with the terms of the 1982 Nuclear Waste Policy Act. The PGE contract with DOE, "Standard Contract for Disposal of Spent Nuclear Fuel and/or High-Level Radioactive Waste," provides the basis for the schedule forecast in DOE's annual acceptance priority ranking for receipt of spent nuclear fuel and/or high-level radioactive waste. Previously, the published schedule specified that the first shipment of Trojan spent nuclear fuel was to have been in 2002, and PGE projected the final shipment to be in 2018. Subsequently, the DOE schedule published in July 2004 used 2010 for commencing Repository operations and changed the first shipment date for Trojan fuel to 2013. This schedule did not specify a projected date for the final Trojan fuel shipment (the schedule covers only 587 of the 791 spent fuel assemblies). PGE projected the July 2004 schedule out to cover the remaining 204 fuel assemblies and arrived at 2023 as being the estimated date of the final shipment. ISFSI radiological decommissioning costs include the cost of removing the MPCs from storage and packaging them for shipment. ISFSI facility decommissioning will occur following the last spent fuel shipment. In February 2007, the DOE established March 2017 as their new key milestone for commencing Repository operations, which was a seven-year delay from year 2010. The DOE's Project Decision Schedule published in January 2009 included a new anticipated date of 2020 for commencing Repository operations, which is an additional three-year delay from year 2017. Using the same modeling assumptions, PGE used this three-year delay in DOE's schedule to project and estimate a new first fuel shipment date of 2023, a final fuel shipment date of 2033, and ISFSI facility decommissioning in 2034. The decommissioning cost estimate and funding plan are based on the assumption that decommissioning will be completed in 2034. This delay in decommissioning will also require continued funding of ISFSI operations and maintenance from the initial projected final fuel shipment date of 2018 through 2033. Annual operations and maintenance costs are estimated at approximately \$3.3 million per year (in 2008 dollars).

9.8.2 TROJAN ISFSI DECOMMISSIONING COST ESTIMATE AND FUNDING PLAN

9.8.2.1 Decommissioning Cost Estimate

Summarizing the results of the Trojan ISFSI cost estimate, Table 9.8-1 provides a breakdown of estimated radiological decommissioning costs based on anticipated decommissioning activities. As indicated in Table 9.8-1, the total cost (in 2008 dollars) for decommissioning the ISFSI is estimated at approximately \$12.6 million. As indicated in Section 9.8.1.2, these expenditures are currently scheduled to require funding from 2023 through 2034 to support packaging of spent fuel for shipment and ISFSI decommissioning.

The cost estimate was prepared using the guidance in NUREG-1757, Consolidated NMSS Decommissioning Guidance, Financial Assurance, Recordkeeping, and Timeliness, Section A.3.1, Preparing the Cost Estimate.



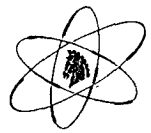
In accordance with 10 CFR 72.30(b), the Trojan ISFSI decommissioning cost estimate and associated funding levels are adjusted over the life of the ISFSI as determined to be necessary as part of and on a schedule consistent with Oregon Public Utility Commission (OPUC) rate cases. Since decommissioning of the ISFSI primarily consists of transferring the contents of the sealed MPCs to an off-site facility for final disposal or storage (see Section 9.8.1.1), decommissioning cost estimate adjustments likely would be necessary only upon receipt of any new information indicating that the current co-owner funding levels are no longer adequate to cover decommissioning costs. Such information could include major changes to the timing of decommissioning and associated decommissioning fund expenditures, the scope of Transport Cask loading operations, and/or DOE repository receipt requirements.

9.8.2.2 Decommissioning Funding Plan

Each of the Trojan ISFSI co-owners separately collects through rates the funds for the decommissioning of the Trojan ISFSI. PGE and PP&L deposit these funds in external trust funds in accordance with 10 CFR 50.75(e)(1)(ii) (Reference 5) as allowed by 10 CFR 72.30(c)(5) (Reference 1) together with an NRC partial exemption dated March 17, 2005. (Reference 7). The BPA provides EWEB's portion of Trojan ISFSI decommissioning funds as necessary as described in Section 9.8.2.2.2. Each co-owner maintains a decommissioning fund collection schedule which ensures that sufficient funds are collected and available to fully fund its portion of total decommissioning activity expenditures. As discussed above, in accordance with 10 CFR 72.30(b), the Trojan ISFSI co-owners periodically assess and adjust, as necessary, the financial assurance amount required to complete Trojan ISFSI decommissioning. The manner in which each co-owner provides funding and financial assurance for Trojan ISFSI decommissioning is detailed below.

9.8.2.2.1 PGE Funding

As a majority co-owner in the Trojan ISFSI, PGE is responsible for funding 67.5 percent of the total ISFSI decommissioning costs specified in Section 9.8.2.1. As allowed by 10 CFR 72.30(c)(5) and a related NRC partial exemption (Reference 7), PGE provides ISFSI decommissioning funding assurance using the method of 10 CFR 50.75(e)(1)(ii). Specifically, PGE has established and maintains an external sinking fund in the form of a trust, which is segregated from PGE's assets and outside PGE's administrative control, and into which funds are periodically set aside such that the total amount of funds will be sufficient to pay decommissioning costs. As allowed by 10 CFR 50.75(e)(1)(ii)(A) for licensees such as PGE that recover the total estimated decommissioning costs through ratemaking regulation, this method is the exclusive mechanism that PGE relies upon to provide financial assurance for Trojan ISFSI decommissioning. In accordance with the NRC partial exemption dated March 17, 2005 (Reference 7), in the future, if funds remaining to be placed into PGE's external sinking fund to cover PGE's 67.5 percent ownership share of Trojan ISFSI decommissioning costs are no longer approved for recovery in rates by a competent rate regulating authority (currently OPUC), the subject exemption will be considered no longer effective. In such an event, PGE would no



longer be allowed to use the financial assurance mechanisms of 10 CFR 50.75(e), but rather would be required to use financial assurance methods as specified in 10 CFR 72.30(c).

9.8.2.2.2 EWEB/BPA Funding

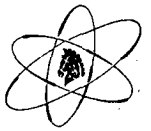
BPA is obligated through Net Billing Agreements to fund EWEB's 30 percent share of the total Trojan ISFSI decommissioning costs as specified in Section 9.8.2.1. As allowed by 10 CFR 72.30(c)(4), BPA, as a Federal government entity fulfilling the decommissioning funding obligations of EWEB, a licensee, provides financial assurance in the form of a statement of intent. The statement of intent contains a reference to the Trojan ISFSI decommissioning cost estimate, indicating that funds for radiological decommissioning of the Trojan ISFSI will be obtained when necessary.

9.8.2.2.3 PP&L Funding

PP&L is responsible for funding its share – 2.5 percent – of the total ISFSI decommissioning costs specified in Section 9.8.2.1. As allowed by 10 CFR 72.30(c)(5) and a related NRC partial exemption (Reference 7), PP&L provides ISFSI decommissioning funding assurance using the method of 10 CFR 50.75(e)(1)(ii). Specifically, PP&L has established and maintains an external sinking fund in the form of a trust, which is segregated from PP&L's assets and outside PP&L's administrative control, and into which funds are periodically set aside such that the total amount of funds will be sufficient to pay decommissioning costs. As allowed by 10 CFR 50.75(e)(1)(ii)(A) for licensees such as PP&L that recover the total estimated decommissioning costs through ratemaking regulation, this method is the exclusive mechanism that PP&L relies upon to provide financial assurance for Trojan ISFSI decommissioning. In accordance with the NRC partial exemption dated March 17, 2005 (Reference 7), in the future, if funds remaining to be placed into PP&L's external sinking fund to cover PP&L's 2.5 percent ownership share of Trojan ISFSI decommissioning costs are no longer approved for recovery in rates by a competent rate regulating authority (currently OPUC), the subject exemption will be considered no longer effective. In such an event, PP&L would no longer be allowed to use the financial assurance mechanisms of 10 CFR 50.75(e), but rather would be required to use financial assurance methods as specified in 10 CFR 72.30(c).

9.8.3 RECORD KEEPING FOR DECOMMISSIONING

Records of information important to the safe and effective decommissioning of the ISFSI will be maintained for the life of the ISFSI. The types of information that will be maintained as records for decommissioning are listed in 10 CFR 72.30(d).



9.10 REFERENCES

1. Code of Federal Regulations, Title 10, Part 72.30, "Financial Assurance and Recordkeeping for Decommissioning."
2. Code of Federal Regulations, Title 10, Part 72.130, "Criteria for Decommissioning."
3. NUREG-1757, "Consolidated NMSS Decommissioning Guidance, Financial Assurance, Recordkeeping, and Timeliness," Section A.3.1, "Preparing the Cost Estimate".
4. Deleted in Revision 9.
5. Code of Federal Regulations, Title 10, Part 50.75, "Reporting and Recordkeeping for Decommissioning Planning."
6. PGE-8010, "Portland General Electric (PGE) Nuclear Quality Assurance Program for Trojan Independent Spent Fuel Storage Installation (10 CFR 72) Operations and Radioactive Material Packaging and Transportation (10 CFR 71) Activities," a.k.a., Trojan Nuclear Quality Assurance Program.
7. U.S. Nuclear Regulatory Commission letter, "Partial Conditional Exemption from the Requirements of 10 CFR 72.30(c)(5)," dated March 17, 2005.
8. U.S. Nuclear Regulatory Commission letter, "Termination of Trojan Nuclear Plant Facility Operating License No. NPF-1," dated May 23, 2005.



TABLE 9.8-1
ISFSI Radiological Decommissioning Costs

ACTIVITY	ESTIMATED COST (thousands of 2008 dollars)
Preparation for Spent Fuel Transfer	410
Spent Fuel Transfer	7,173
Characterization	57
Decontamination and Disposal ¹	508
Final Status Survey	1,401
PGE Staff (post-fuel transfer)	549
Sub-Total (without contingency)	10,098
Contingency (25%)	2,525
<hr/> Total Radiological Decommissioning Cost	<hr/> 12,623

¹ Assumes separate burial of one Concrete Cask as Low Level Radioactive Waste.